Polymer 51 (2010) 2177–2184

Contents lists available at ScienceDirect

Polymer

journal homepage: www.elsevier.com/locate/polymer

Layered-silicate based polystyrene nanocomposite microcellular foam using supercritical carbon dioxide as blowing agent

Bin Zhu, Weibin Zha, Jintao Yang, Cailiang Zhang, L. James Lee*

Department of Chemical and Biomolecular Engineering, The Ohio State University, Columbus, OH 43210, USA

ARTICLE INFO

Article history:
Received 25 December 2009
Received in revised form
8 March 2010
Accepted 13 March 2010
Available online 24 March 2010

Keywords:
Expandable polystyrene
Layered-silicate
Microcellular

ABSTRACT

Exfoliated layered-silicate in the polystyrene (PS) block copolymer with different molecular weights was employed as a model material to investigate the PS nanocomposite microcellular foams expanded by supercritical carbon dioxide. Using a well-controlled foaming procedure, we investigated the influence of molecular weight of PS, dispersion and loading of layered-silicate and pressure drop rate of a blowing agent on the cell size and cell density. Our experimental results indicate that only exfoliated layered-silicate can inhibit the cell expansion and has high nucleation efficiency during foaming. The average cell diameter can be reduced from 6 μm to 1.4 μm and the cell density can be increased from 7.6×10^9 cells/cm^3 to 5.0×10^{11} cells/cm^3. On the contrary, aggregated layered-silicate in PS did not show any effect on the cell morphology of PS foam.

1. Introduction

Polymer microcellular foams usually refer to foams with an average cell diameter smaller than 10 μm and cell density higher than 10^8 cells/cm^3 [1]. Due to its ultra small cell size and high cell density, the microcellular foams have light weight and can provide better thermal insulation and acoustic properties compared to solid materials without sacrificing too much mechanical strength. A successful manufacturing process of making microcellular foams requires a high pressure drop and fast cooling rate to provide high nucleant density, a low bubble growth rate and less bubble coalescence during foaming to control the cell size and cell density [1–5]. Adding heterogeneous nucleation agents such as inorganic particles or block copolymer micelles into the polymer matrix is very helpful for preparing microcellular foams [2,6–13]. Nanoparticles which have a high specific surface area should be very efficient in nucleation. However, if nanoparticles are not uniformly dispersed, their nucleation efficiency would be significantly inhibited. In this study, we carried out a series of well-controlled batch foaming experiments to investigate the influence of layered-silicate and CO_2 pressure drop rate on the cell size and cell density. The experimental procedure was similar to that reported by Ema et al. [2]. Standford et al. [4] investigated polystyrene (PS) foaming using supercritical carbon dioxide (CO_2). Their results showed that the cell size and cell density of PS foams are independent of molecular weight and polydispersity of PS. However, the cell size of commercial PS foam was found to be much larger because of the low molecular weight ingredients in the resin. In order to eliminate this contamination effect in our study, we used ionic polymerization to synthesize PS with controlled molecular weight and low polydispersity.

CO_2 in the supercritical state is an inexpensive, safe and environmentally benign blowing agent [14]. When PS is saturated with supercritical CO_2 under high pressure, its glass transition temperature (T_g) and shear viscosity decrease [15–19], making the polymer relatively easy to process. A layered-silicate, montmorillonite (MMT), with a thickness of 1 nm and lateral dimension of 100–200 nm, is used as a heterogeneous nucleation agent [20]. The dispersion of MMT in PS is not easy because the van der Waals force between individual layers makes them very difficult to separate. In this study, we employed a newly developed method to achieve good dispersion of layered-silicate in a PS block copolymer, containing 95 wt.% of PS [21]. This methodology allows up to 20 wt.% of the layered-silicate to be exfoliated uniformly in the polymer matrix. Since the polymer is not covalently bonded to the layered-silicate surface, physical properties of the interface where the heterogeneous nucleation takes place are not affected. The molecular weight of the block copolymer can be chosen across a wide range without affecting the layered-silicate dispersion, enabling us to investigate the influence of molecular weight on cell morphology of this nanocomposite foam.

* Corresponding author. Tel.: +1 614 292 2408; fax: +1 614 292 3947.
E-mail address: leelj@chbmeng.ohio-state.edu (L.J. Lee).

0032-3861/$ – see front matter © 2010 Elsevier Ltd. All rights reserved.
doi:10.1016/j.polymer.2010.03.026

2. Experimental

2.1. Materials

Commercial PS (PS^{COM}, INEOS NOVA PS 1600, $M_n = 104{,}500$ g/mol and $M_w/M_n = 2.61$) was purchased from INEOS NOVA. Organoclay Cloisite® 30B (30B) was provided by Southern Clay Products. 30B is a naturally layered-silicate modified with a quaternary ammonium salt surfactant which has two hydroxyl groups in each molecule. The chemical structure of 30B is shown in Fig. 1, in which the N^+ ion denotes the quaternary ammonium salt and *T* denotes the tallow consisting of 65% C18, 30% C16, and 5% C14. Based on the product bulletin [22], the amount of surfactant residing in the layered-silicate is 30 wt.% determined by an ignition experiment. The mean interlayer gallery spacing of 30B is 1.85 nm characterized by X-ray diffraction (XRD). All other chemicals were purchased from Aldrich and used as received, unless otherwise indicated. The foaming agent CO_2 (>99.9%) was provided by Praxair.

2.2. PS synthesis

All polymers, except the PS^{COM}, used in this study were synthesized by anionic polymerization. A diblock copolymer polystyrene-*block*-poly(2-vinyl pyridine) (PS-*b*-P2VP), which has 5 wt.% of 2-vinyl pyridine block in each polymer chain, was used to exfoliate the layered-silicate by solution mixing. PS with the same molecular weight was also synthesized and mixed with layered-silicate for comparison. A typical commercial PS used for foaming in industry, like INEOS NOVA PS 1600, has a M_n = 100,000 g/mol and $M_w/M_n = 2.61$. Thus, we synthesized PS with three different molecular weights (M_n = 70,000, 140,000 and 210,000 g/mol) in this study.

The synthesis procedure of PS-*b*-P2VP by the sequential anionic polymerization can be found elsewhere [23]. The molecular weights and distributions of block copolymer were determined by Waters gel permission chromatography (GPC) system equipped with a 1515 isocratic HPLC pump and a 2414 differential refractometer. THF was used as the mobile phase with a flow rate of 1 mL/min at 35 °C. The PS standard was used for calibration. The molar ratio of two monomers in the copolymer was characterized by ^{1}H nuclear magnetic resonance (^{1}H NMR, 400 Hz, Bruker TopSpin) spectroscopy.

2.3. Preparation of nanocomposites

PS and PS-*b*-P2VP with different molecular weights (Mn = 70,000, 140,000 and 210,000 g/mol for each) were mixed with 1, 3 and 5 wt.% of layered-silicate in Tetrahydrofuran (THF) using a magnetic stirrer with a stirring rate of 200 rad/s. For the block copolymer which has a M_n of 70,000 g/mol, a much higher amount of layered-silicate, 10–20 wt.%, was also mixed to achieve the lowest foam expansion. It should be noted that the weight percentage of layered-silicate in nanocomposites mentioned in this study is calculated based on the net amount of layered-silicate in 30B, i.e. 70 wt.% [22]. The sample name of the nanocomposite is labeled as follows: (polymer type)-(number average molecular weight)/(wt.% of layered-silicate). For example, if the PS-*b*-P2VP with a M_n of 70,000 g/mol is mixed with 5 wt.% of layered-silicate, the name of this nanocomposite is Block-70k/5-LS. THF was evaporated at 60 °C for 12 h when the polymer and layered-silicate were still under mixing by a magnetic stirrer with a stirring rate of 200 rad/s. Nanocomposites were then further dried in a vacuum oven at 180 °C for 12 h.

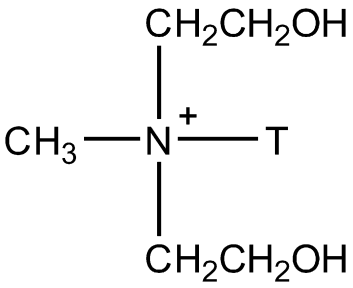

Fig. 1. Chemical structure of 30B surfactant, where *T* is tallow 65% C18, 30% C16, and 5% C14.

Using an X-ray diffractometer (Scintag PAD-V) operated at 45 kV and 20 mA, XRD patterns were obtained to determine the mean interlayer gallery spacing of the plane for various nanocomposites prepared in this study. The wavelength of the X-ray beam (λ) is 0.15406 nm. The range of 2θ scanning of the X-ray intensity employed was 1–12°.

A transmission electron microscope (TEM, FEI technai G2 spirit transmission electron microscope) was used to characterize the dispersion of layered-silicate. Nanocomposite specimens were cut into 50–70 nm via ultra-microtomy at room temperature. The TEM was operated at 120 kv at room temperature.

2.4. Foam preparation

The schematic diagram of the batch foaming setup used in this study is shown in Fig. 2. Polymer nanocomposites were formed into a rod-like shape with a diameter of 2 mm and a length of 15 mm. Then, the sample was placed in a saturation chamber (Swagelok SS-4F-VCR-05) which had a length of 40 mm and an inner diameter of 13 mm. The surface of the inner wall was covered by a Teflon coated aluminum film, which could prevent the sample from sticking on the wall surface. The saturation chamber was immersed in a circulating oil bath heated by a hotplate. A thermometer was placed at the same depth as that of the tank in order to precisely measure the temperature there. All polymer nanocomposite samples were saturated under 13.8 MPa (2000 psi) supercritical CO_2 at 120 °C for 24 h, allowing sufficient time for CO_2 to diffuse into the sample to achieve an equilibrium state. The pressure in the chamber was monitored by a connected pressure gauge and adjusted by an ISCO syringe pump (ISCO 500D Syringe Pump). The CO_2 was released in 0.4, 1.1 and 5.5 s respectively using different gas reducers to make foams by turning off valve #1(Swagelok ss-41s2) and then turning on valve #2 (Swagelok ss-42s4) while the sample in the saturation chamber still remained in the oil bath. Finally, CO_2 in the chamber was released, the chamber was immediately moved into an ice water bath for cooling to fix the cell structure in the foam. Various gas reducers with different inner diameters were connected to the outlet of valve #2 to control the pressure drop rate.

2.5. Characterization of foam morphology

The morphology of foams was examined by a scanning electron microscope (SEM, Phillips XL30). Samples were cryo-fractured in the liquid nitrogen and the fracture surface was sputter-coated with gold. The Scion Image software was used to determine the cell size. For non-circular cells, an equivalent diameter was calculated by assuming that the cells are in circular shape. The cell density in the foam was calculated based on Equation (1) [2], in which $\rho_f\,(g/cm^3)$ is the foam density measured according to ASTM D792, $\rho_p\,(g/cm^3)$ is the density of nanocomposite calculated based on the weight percentage of each component and d (μm) is the average cell diameter.

$$N_c = 10^{12} \times \frac{6\left[1 - \frac{\rho_f}{\rho_p}\right]}{\pi d^3} \quad (\text{cells/cm}^3) \tag{1}$$

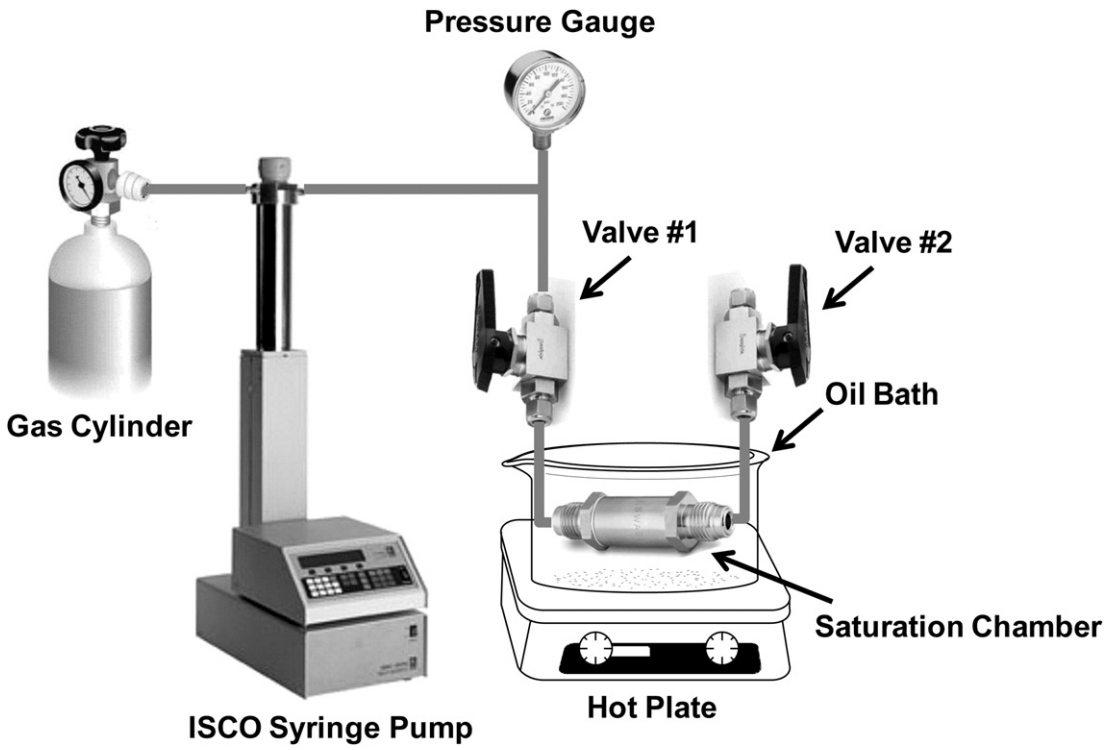

Fig. 2. Schematic diagram of the batch foaming setup employed in this study.

3. Results and discussion

3.1. Dispersion of layered-silicate in different polymer matrix

Since PS is incompatible with the layered-silicate, we synthesized PS-*b*-P2VP diblock copolymers to achieve good dispersion. The entire block copolymer can be end-tethered on the layered-silicate surface by the ion–dipole interaction between the positively charged N^+ ions in the surfactant residing at the surface of the layered-silicate and the dipoles in the P2VP block of PS-*b*-P2VP diblock copolymers [21]. To avoid making any significant change on the structure and the physical properties of PS, only 5 wt.% of 2VP was used in the copolymer.

The XRD patterns of polymer/LS nanocomposites prepared in this study are shown in Fig. 3. Fig. 3(a) is the XRD pattern of pristine 30B, which has a peak at $2\theta = 4.7^\circ$. According to Bragg's equation $n\lambda = 2d\times\sin\theta$, in which the wavelength $\lambda = 0.15406$ nm, the average interlayer gallery spacing d can be calculated as ~1.86 nm. When 1 wt.% of layered-silicate in 30B was mixed with PS-70k in THF, there was a peak at $2\theta = 5.7^\circ$ indicating the aggregated layered-silicate in PS (Fig. 3(b)). The average interlayer gallery spacing d is 1.56 nm which is smaller than that of pristine 30B. In order to explain this, 30B was mixed with THF without PS and then filtrated and dried under vacuum. The XRD pattern showed the same result as that in Fig. 3(a). The thermogravimetric analysis (TGA) indicated that the surfactant content on the layered-silicate surface was still 30 wt.%, the same as the original 30B. Thus, we conclude that the surfactant on the layered-silicate surface has not been washed away by THF. All other samples made from PS and 30B showed very similar XRD patterns as Fig. 3(b) indicating poor dispersion of layered-silicate in PS. The XRD results are further confirmed by TEM images. Fig. 4(a)–(c) are the TEM images of PS-70k mixed with 1, 3, 5 wt.% of layered-silicate, respectively. All images show that the layered-silicate is aggregated together forming tactoids with

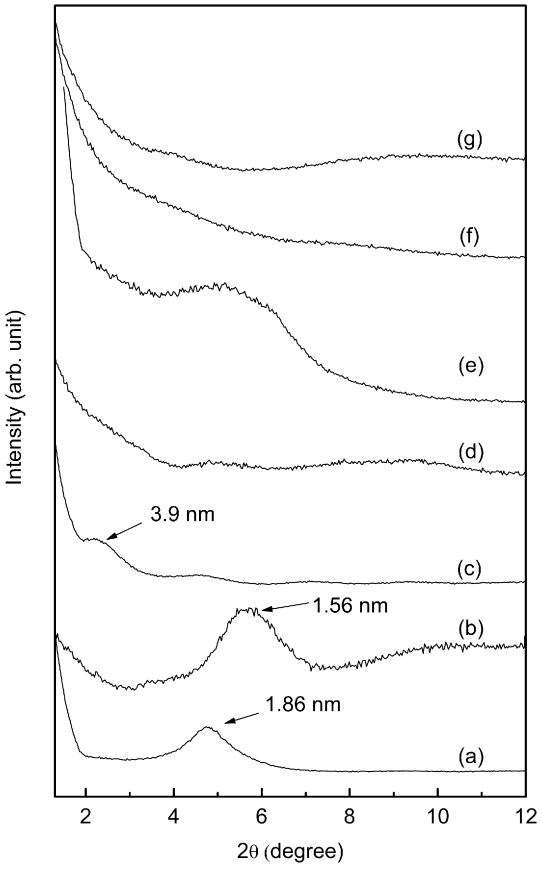

Fig. 3. XRD patterns of nanocomposites: (a) pristine 30B; (b) PS-70k/1-LS; (c) Block-210k/5-LS (d) Block-140k/5-LS; (e) Block-70k/20-LS; (f) Block-70k/10-LS; (g) Block-70k/5-LS.

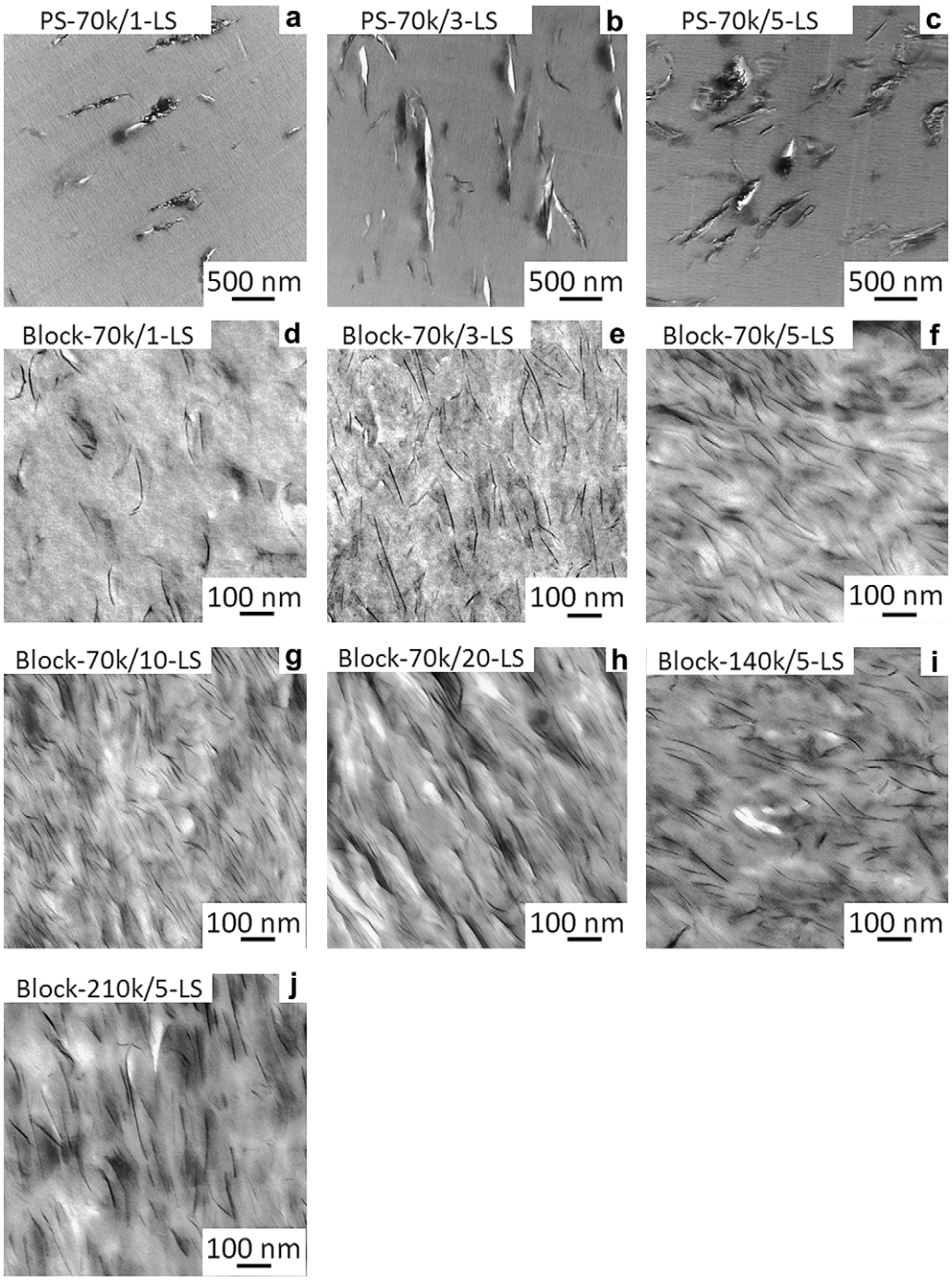

Fig. 4. TEM images for nanocomposites: (a) PS-70k/1-LS; (b) PS-70k/3-LS; (c) PS-70k/5-LS; (d) Block-70k/1-LS; (e) Block-70k/3-LS; (f) Block-70k/5-LS; (g) Block-70k/10-LS; (h) Block-70k/20-LS; (i) Block-140k/5-LS; (j) Block-210k/5-LS.

a thickness of tens of nanometers in the PS matrix. Comparing Fig. 4 (a), (b) and (c), one can observe that adding different amounts of layered-silicate in PS only changes the number of tactoids but not the size of them.

Fig. 3(c)–(g) are the XRD patterns of PS-*b*-P2VP mixed with 30B. The disappearance of peaks in the XRD pattern indicates the exfoliation of layered-silicate in the block copolymer. Fig. 3(c), (d) and (g) are the XRD patterns of 5 wt.% layered-silicate mixed with block copolymers with different molecular weights, i.e. Block-210k, Block-140k and Block-70k. There is only one peak appearing in Fig. 3(c) at $2\theta = 2.9^{\circ}$ corresponding to an average interlayer gallery spacing of 3.9 nm. This indicates that the layered-silicate can be dispersed better in a low molecular weight block copolymer because the small molecule is easier to diffuse into the interlayer gallery. For the Block-70k, the maximum amount of layered-silicate exfoliated is between 10 and 20 wt.% as shown in Fig. 3(f) and (e). The XRD results of block copolymer mixed with 30B were further confirmed by TEM images. Fig. 4(d)–(h) are TEM images of different amounts of layered-silicate in Block-70k. Fig. 4(e) and (f) show the samples of 5 and 10 wt.% of layered-silicate in Block-70k. The layered-silicate was exfoliated and uniformly dispersed in all samples. Fig. 4(h) is the TEM image of Block-70k/20-LS. Even at

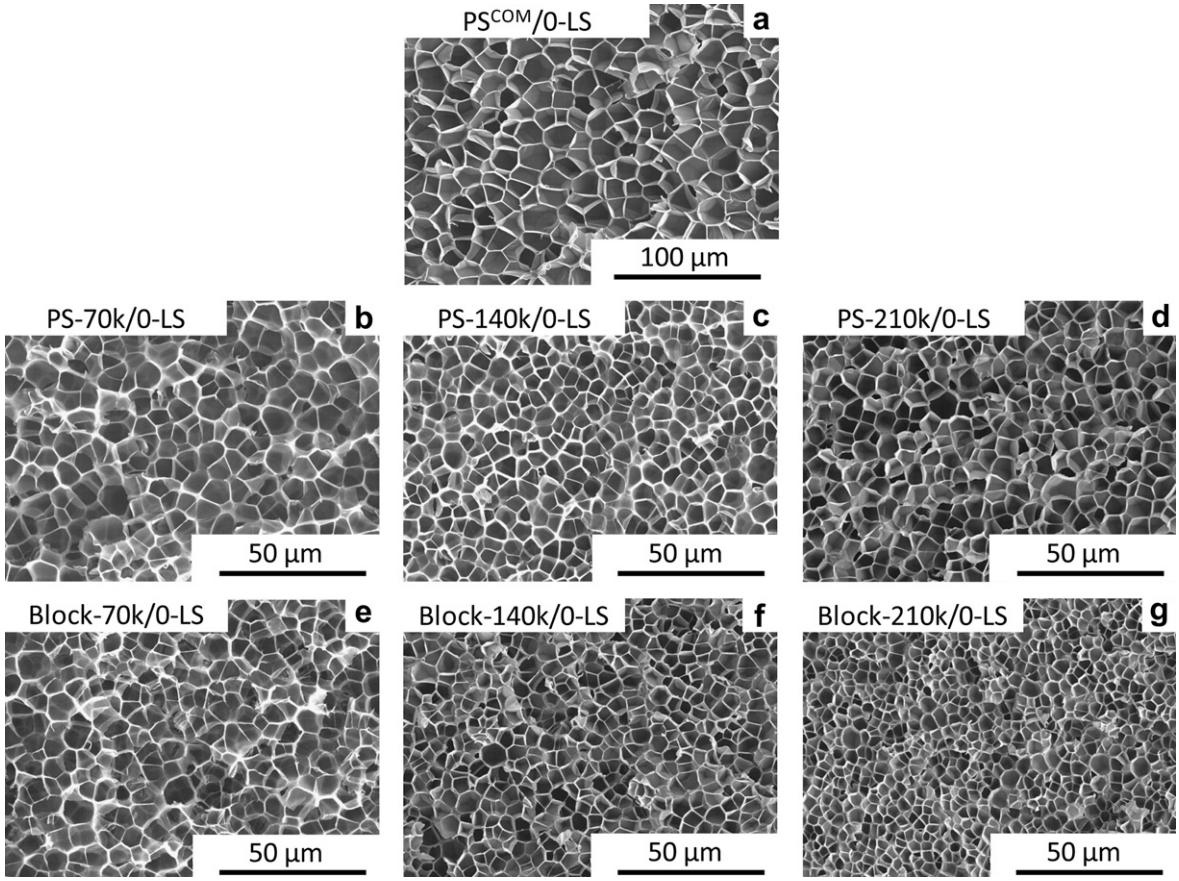

Fig. 5. SEM images of PS^{COM}, PS and PS-b-P2VP foams without layered-silicate: (a) PS^{COM}/0-LS; (b) PS-70k/0-LS; (c) PS-140k/0-LS; (d) PS-210k/0-LS; (e) Block-70k/0-LS; (f) Block-140k/0-LS; (g) Block-210k/0-LS.

such a high loading, most layered-silicate was well dispersed and only a few aggregates in the polymer matrix corresponding to the peak were observed in the XRD pattern (i.e. Fig. 3(e)). We, therefore, conclude that exfoliated layered-silicate can be obtained in PS-*b*-P2VP.

3.2. Cell morphology of PS and PS-b-P2VP foams without layered-silicate

The SEM images of cell morphology for foams without layered-silicate are shown in Fig. 5. The average cell diameter and cell density are listed in Table 1. The cell size of PS^{COM} foam, which is about 14.4 μm, is obviously larger than the cell size of anionic polymerized PS foams as reported by Stafford et al. [4].

PS-*b*-P2VPs with the same molecular weight as the anionic polymerized PS samples were also made into foams using the same foaming condition and procedure mentioned above. The pressure drop time for making polymer foams is 0.4 s. The SEM images of cell morphology are shown in Fig. 5 and the average cell diameter and cell density are listed in Table 1. The average cell diameter of PS foams decreased slightly from 6.6 to 5.7 μm when the molecular weight of PS increased from 70 k to 210 k. However, the cell size of PS-*b*-P2VP foams showed obvious dependence on the molecular weight. The average cell diameter decreased from 6.0 to 3.7 μm when the molecular weight of the block copolymer increased from 70 k to 210 k. Comparing the foams made from PS and PS-*b*-P2VP with the same molecular weight, the cell sizes of PS-*b*-P2VP foams are smaller than the ones of PS foams and the difference becomes increasingly larger when the molecular weight increases. One hypothesis is that PS-*b*-P2VP can form a microphase separated structure at higher molecular weight [24]. The dispersed phase in the polymer matrix has a heterogeneous nucleation effect causing the cell size to decrease and the cell density to increase comparing to homopolymer foams [8]. However, our rheological study of Block-210k showed no microphase separated structure in the block copolymer. Since the addition of CO_2 does not make PS and P2VP more immiscible, we expect that the block copolymer is in a disorder state when saturated with CO_2 at 120 °C. It has been reported that the solubility of CO_2 in P2VP is much higher than in PS [25]. When the polymer was saturated with CO_2 under 1500 psi at 35 °C, 100 g PS could absorb 5.56 g CO_2 but 100 g P2VP can absorb 17.9 g CO_2. The reason is that the nitrogen atom on P2VP renders the polymer somewhat basic and it therefore interacts more favorably with the slightly acidic CO_2 molecules than with PS [25]. A higher concentration of CO_2 in PS-*b*-P2VP is beneficial for

Table 1
Average cell diameter and cell density of PS foams without layered-silicate in polymers.

Polymer Type	M_n (g/mol)	Average Cell Diameter (μm)	Cell Density (cells/cm3)
PS^{COM}	104 500	14.4 ± 2.3	5.7×10^8
PS-70k/0-LS	70k	6.6 ± 1.3	5.6×10^9
PS-140k/0-LS	14k	5.1 ± 0.9	1.2×10^{10}
PS-210k/0-LS	210k	5.7 ± 1.0	8.9×10^9
Block-70k/0-LS	70k	6.0 ± 1.3	7.6×10^9
Block-140k/0-LS	14k	4.5 ± 1.1	1.8×10^{10}
Block-210k/0-LS	210k	3.7 ± 0.6	3.1×10^{10}

increasing the nucleation rate, creating more cells and reducing the cell size. The second explanation seems to be more reasonable in our study.

3.3. Effect of layered-silicate loading and dispersion on cell morphology

PS and PS-*b*-P2VP were mixed with predetermined amounts of layered-silicate to make nanocomposites, which were later saturated with CO_2 under 2000 psi at 120 °C for 24 h. The pressure drop time for making nanocomposite foams was 0.4 s. SEM images of cell morphologies are shown in Fig. 6, in which PS-70k/LS foams are compared with Block-70k/LS foams. Adding layered-silicate up to 5 wt.% in PS did not change cell size of PS-70k/LS foams. In comparison, the cell size of Block-70k/LS foams showed clear dependence on the layered-silicate loading. The cell size became smaller when more layered-silicate was mixed with the block copolymer. With 20 wt.% of layered-silicate in the block copolymer, the average cell diameter could be reduced to about 1.4 μm, which is the smallest cell size observed under these foaming conditions.

Fig. 7 summaries the average cell diameter and cell density of all polymer nanocomposite foams prepared in this study. In Fig. 7(a) and (b), we find that adding up to 5 wt.% of layered-silicate in the polymer matrix has no effect on the PS foam cell size and cell density. The molecular weight of PS seems to have a more significant effect on the cell morphology. Foams with a higher molecular weight of PS have a smaller cell size and higher cell density. One explanation is that the higher molecular weight PS is more viscous, inhibiting the cell expansion and coalescence during foaming. However, this dependence becomes insignificant when the molecular weight of PS is larger than 100,000 g/mol.

On the other hand, the cell size and cell density of foams show clear dependence on the layered-silicate loading when the layered-silicate is exfoliated in the PS-*b*-P2VP matrix. In Fig. 7(c) and (d), the average cell diameter decreases and cell density increases when more layered-silicate is added. It is obvious that the dispersion of layered-silicate in the polymer matrix plays an important role in controlling the cell morphology during the foaming process. As TEM images and XRD patterns showing in Figs. 3 and 4 suggested, the layered-silicate is exfoliated in the PS-*b*-P2VP up to 20 wt.% but is aggregated in the PS. During the cell expansion, the layered-silicate is forced to re-align along the cell wall. The confined polymer chains and the orientation of the plate-like layered-silicate cause the viscosity of nanocomposite to increase. Therefore, the cell expansion and coalescence is inhibited. However, when the polymer matrix itself becomes more viscous due to the increase of molecular weight, the enhancement of viscosity from the layered-silicate becomes less obvious [21]. There is a threshold value of layered-silicate loading above which the cell morphology of PS-*b*-P2VP/LS foams is affected significantly. In Fig. 7(c) and (d), we find that the cell size and cell density of all PS-*b*-P2VP/LS foams do not change much with a loading of 1 wt.% of layered-silicate, but changed significantly with 3 wt.% layered-silicate. The TEM images in Fig. 4 shows that only a small portion of polymer chains are end-tethered onto the layered-silicate surface at 1 wt.% of layered-silicate loading. Most polymer chains can still move easily during cell expansion. However, when the layered-silicate loading is increased to 3 wt.%, most polymer chains are end-tethered onto

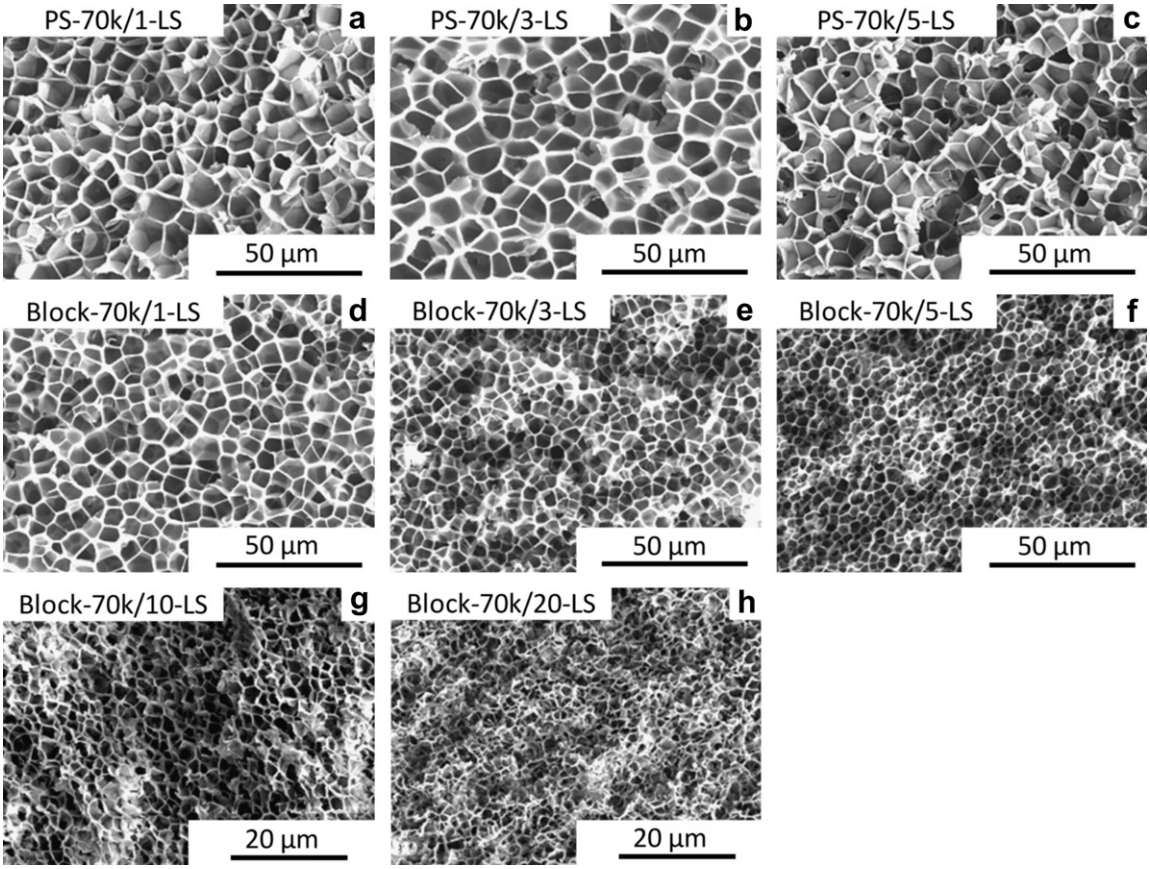

Fig. 6. SEM images of PS/LS and Block/LS nanocomposites foams: (a) PS-70k/1-LS; (b) PS-70k/3-LS; (c) PS-70k/5-LS; (d) Block-70k/1-LS; (e) Block-70k/3-LS; (f) Block-70k/5-LS; (g) Block-70k/10-LS; (h) Block-70k/20-LS.

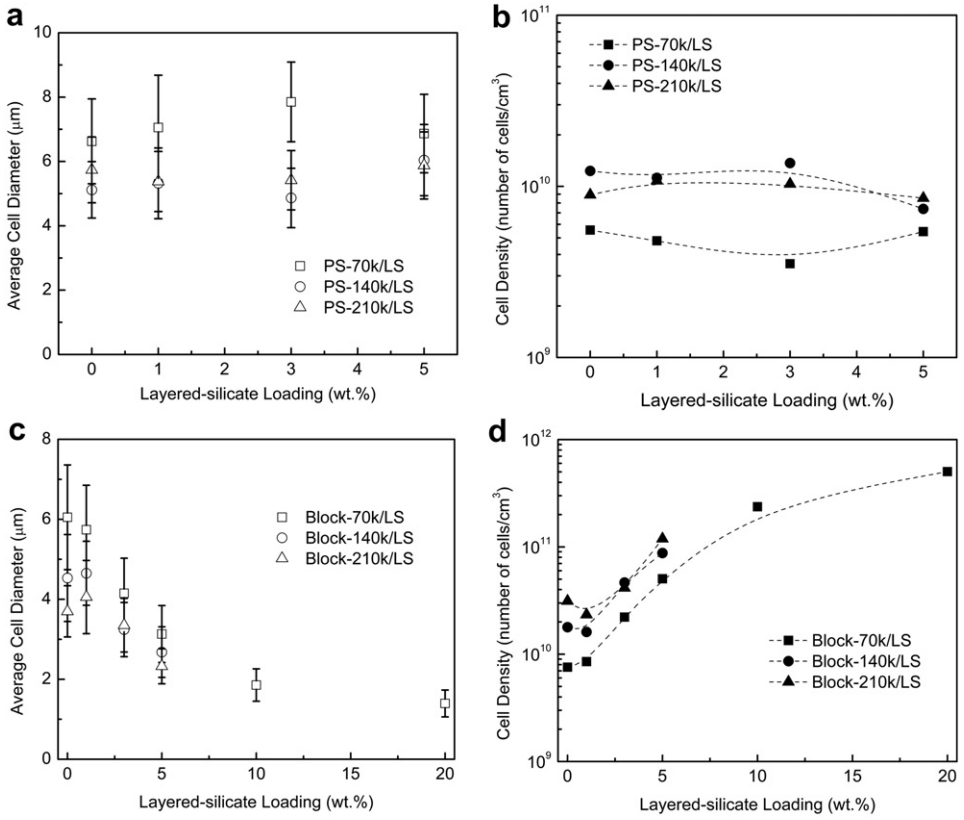

Fig. 7. Average cell diameter (a) and cell density (b) of PS foams influenced by layered-silicate loading. Average cell diameter (c) and cell density (d) of block copolymer foams influenced by layered-silicate loading.

the layered-silicate surface causing a significant increase of nanocomposite viscosity. Moreover, individual layers and tactoids of layered-silicate may form a percolated network in which the layered-silicate is confined at its original position. Therefore, we are able to observe a significant influence on cell morphology when 3 wt.% of layered-silicate is added. Furthermore, better dispersion generates more heterogeneous nucleation sites at the same loading of layered-silicate.

3.4. Effect of pressure drop rate on cell morphology

It has been reported that the pressure drop rate is a significant factor for making polymer microcellular foams [3]. A higher pressure drop rate leads to a smaller cell size and a higher cell density. In our study, a series of gas reducers were used to adjust the pressure drop rate. The total pressure drop time can be adjusted from 0.4, 1.1 to 5.5 s. Block-70k mixed with different amounts of layered-silicate was made into polymer nanocomposite foams using different pressure drop rates. The average cell diameter and cell density are summarized in Fig. 8. As expected, the average cell diameter decreased and the cell density increased when the pressure drop rate increased. When the pressure drop rate was high, more CO_2 molecules participated in the nucleation and less CO_2 molecules diffused into the existed cells, therefore inhibiting the cell expansion. Once the layered-silicate was added in the polymer matrix as a heterogeneous nucleation agent, the energy barrier for nucleation was lower compared to that in pure PS. Thus, CO_2 was relatively easy to nucleate near the surface of layered-silicate and

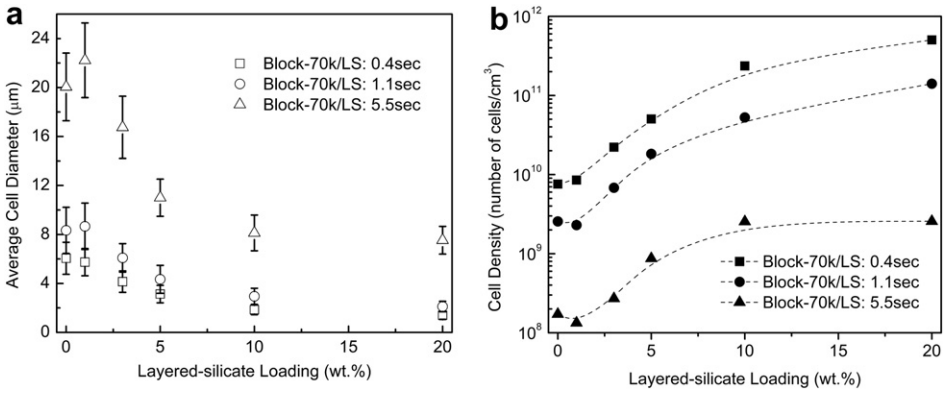

Fig. 8. Average cell diameter (a) and cell density (b) of Block-70k/LS foams influenced by the pressure drop rate.

the cell density increased. At a pressure drop time of 5.5 s, the average cell diameter for pure block copolymer was about 20 μm. After it was mixed with 10 wt.% of layered-silicate, the average cell diameter decreased to 8 μm and the cell density increased to 2.6×10^9 cells/cm^3.

In practice, it is difficult to achieve very high pressure drop rates in the foaming process. Thus, adding exfoliated nanoparticles as a heterogeneous nucleation agent is an effective way to produce microcellular foams.

4. Conclusions

We demonstrated that up to 20 wt.% of layered-silicate could be exfoliated in a series of PS-*b*-P2VP with different molecular weights. Using a well-controlled foaming procedure, our experimental results showed that only exfoliated layered-silicate could inhibit the cell expansion and increased the cell density in the PS foams. On the contrary, aggregated layered-silicate did not influence the cell size and cell density at all. With an increased amount of exfoliated layered-silicate mixed with PS-*b*-P2VP, the cell size could be further reduced to 1.4 μm and the cell density could be increased to 5×10^{11} cells/cm^3. We controlled the pressure drop at different rates and observed that a higher pressure drop rate was also significant to prepare microcellular foams. At different pressure drop rates, exfoliated layered-silicate was still effective in cell size control.

References

[1] Arora KA, Lesser AJ, McCarthy TJ. Macromolecules 1998;31:4614–20.
[2] Ema Y, Ikeya M, Okamoto M. Polymer 2006;47:5350–9.
[3] Guo QP, Wang J, Park CB, Ohshima M. Industrial & Engineering Chemistry Research 2006;45:6153–61.
[4] Stafford CM, Russell TP, McCarthy TJ. Macromolecules 1999;32:7610–6.
[5] Siripurapu S, Coughlan JA, Spontak RJ, Khan SA. Macromolecules 2004;37:9872–9.
[6] Shen J, Zeng CC, Lee LJ. Polymer 2005;46:5218–24.
[7] Zeng C, Han X, Lee LJ, Koelling KW, Tomasko DL. Advanced Materials (Weinheim, Germany) 2003;15:1743–7.
[8] Spitael P, Macosko CW, McClurg RB. Macromolecules 2004;37:6874–82.
[9] Siripurapu S, DeSimone JM, Khan SA, Spontak RJ. Macromolecules 2005;38:2271–80.
[10] Li L, Yokoyama H, Nemoto T, Sugiyama K. Advanced Materials 2004;16:1226–9.
[11] Yokoyama H, Li L, Nemoto T, Sugiyama K. Advanced Materials 2004;16:1542–6.
[12] Yokoyama H, Sugiyama K. Macromolecules 2005;38:10516–22.
[13] Han XM, Shen J, Huang HX, Tomasko DL, Lee LJ. Polymer Engineering and Science 2007;47:103–11.
[14] Sato Y, Iketani T, Takishima S, Masuoka H. Polymer Engineering and Science 2000;40:1369–75.
[15] Zhang ZY, Handa YP. Journal of Polymer Science Part B-Polymer Physics 1998;36:977–82.
[16] Wissinger RG, Paulaitis ME. Industrial & Engineering Chemistry Research 1991;30:842–51.
[17] Alessi P, Cortesi A, Kikic I, Vecchione F. Journal of Applied Polymer Science 2003;88:2189–93.
[18] Pantoula M, Panayiotou C. Journal of Supercritical Fluids 2006;37:254–62.
[19] Wingert MJ, Shukla S, Koelling KW, Tomasko DL, Lee LJ. Industrial & Engineering Chemistry Research 2009;48:5460–71.
[20] Ray SS, Okamoto M. Progress in Polymer Science 2003;28:1539–641.
[21] Zha WB, Han CD, Han SH, Lee DH, Kim JK, Guo MM, et al. Polymer 2009;50:2411–23.
[22] Cloisite® 30B Typical Physical Properties Bulletin.
[23] Matsushita Y, Shimizu K, Nakao Y, Choshi H, Noda I, Nagasawa M. Polymer Journal 1986;18:361–6.
[24] Schulz MF, Khandpur AK, Bates FS, Almdal K, Mortensen K, Hajduk DA, et al. Macromolecules 1996;29:2857–67.
[25] Zhang Y, Gangwani KK, Lemert RM. Journal of Supercritical Fluids 1997;11:115–34.